climate

MDPI

Article

Quantifying Aggravated Threats to Stormwater Management Ponds by Tropical Cyclone Storm Surge and Inundation under Climate Change Scenarios

Hongyuan Zhang [1], Dongliang Shen [1], Shaowu Bao [1,*], Leonard Pietrafesa [1,2], Paul T. Gayes [1] and Hamed Majidzadeh [3]

[1] Department of Marine Science, Coastal Carolina University, Conway, SC 29528, USA
[2] Department of Marine, Earth, Atmospheric Sciences, North Carolina State University, Raleigh, NC 27695, USA
[3] South Carolina Sea Grant Consortium, Charleston, SC 29401, USA
* Correspondence: sbao@coastal.edu

Abstract: Stormwater management ponds (SMPs) protect coastal communities from flooding caused by heavy rainfall and runoff. If the SMPs are submerged under seawater during a tropical cyclone (TC) and its storm surge, their function will be compromised. Under climate change scenarios, this threat is exacerbated by sea level rise (SLR) and more extreme tropical cyclones. This study quantifies the impact of tropical cyclones and their storm surge and inundation on South Carolina SMPs under various SLR scenarios. A coupled hydrodynamic model calculates storm surge heights and their return periods using historical tropical cyclones. The surge decay coefficient method is used to calculate inundation areas caused by different return period storm surges under various SLR scenarios. According to the findings, stormwater management ponds will be aggravated by sea level rise and extreme storm surge. In South Carolina, the number of SMPs at risk of being inundated by tides and storm surges increases almost linearly with SLR, by 10 SMPs for every inch of SLR for TC storm surges with all return periods. Long Bay, Charleston, and Beaufort were identified as high-risk coastal areas. The findings of this study indicate where current SMPs need to be redesigned and where more SMPs are required. The modeling and analysis system used in this study can be employed to evaluate the effects of SLR and other types of climate change on SMP facilities in other regions.

Keywords: stormwater management ponds; tropical cyclones; sea level rise; hydrodynamic model; South Carolina

Citation: Zhang, H.; Shen, D.; Bao, S.; Pietrafesa, L.; Gayes, P.T.; Majidzadeh, H. Quantifying Aggravated Threats to Stormwater Management Ponds by Tropical Cyclone Storm Surge and Inundation under Climate Change Scenarios. *Climate* **2022**, *10*, 157. https://doi.org/10.3390/cli10100157

Academic Editor: Daniele Bocchiola

Received: 21 September 2022
Accepted: 17 October 2022
Published: 21 October 2022

1. Introduction

Tropical cyclones (TCs) threaten coastal communities with flooding, including both freshwater flash floods caused by heavy rain and seawater inundation caused by storm surges. Stormwater management ponds (SMP), including both (wet) retention ponds which hold water year-round and (dry) detention ponds which only hold water for a short time before the water enters streams, are a critical type of infrastructure that protects coastal communities from flood hazards caused by heavy rainfalls and runoff. A study in southwestern Taiwan showed that detention ponds reduce the inundated potential, inundated volume, flood damage, and flood stage of peak flow [1]. Sahoo and Pekkat [2] found that detention ponds reduce the effect of urban flood in an urbanizing catchment, reducing flood depth by 46.5% and the inundated area by 43%. Similarly, Chrétien et al. [3] analyzed retention ponds in a small agricultural catchment of Canada and stated that retention ponds could reduce peak flows by 38%.

Retention ponds fail to function when the rainfall exceeds the pond's capacity, e.g., with the underprediction of rainfall intensity or unrealistic predictions of post-development

flows [4]. Similarly, during TC-induced coastal compound flooding, the function of retention ponds will fail to retain rainfall runoff water if they are submerged by seawater inundation.

Under climate change scenarios, the projected sea level rise (SLR) and more extreme storms in the future will pose aggravated threats to the proper functioning of SMPs.

Since the last glacial period ended about 15,000 years ago [5,6], global temperature rises have caused the thermal expansion of seawater and glacial ice melting, resulting in sea level rise and increased land surface runoff, respectively [5,7]. Although studies on exact sea level trends are subject to uncertainty [8,9], most coastal areas around the world have experienced and continue to experience sea level rise periods. Depending on the volume of greenhouse gases to be emitted in the coming years, the Representative Concentration Pathway (RCP), which is a greenhouse gas concentration trajectory, is used by IPCC to evaluate climate change scenarios [10]. According to three different projections in the latest IPCC report, the global average sea level rise in 2100 may be 0.43 m (likely range: 0.29–0.59 m), 0.55 m (likely range: 0.39–0.72 m), or as much as 0.84 m (likely range: 0.61–1.10 m) under RCP2.6, RCP4.5, and RCP8.5, respectively. Griffiths et al. [11] projected that ninety percent of the coastal areas will experience a sea level rise of more than 0.2 m if global warming exceeds two degrees Celsius above pre-industrial levels. Parris et al. [12] predicted sea level rise of 0.2 m (lowest), 0.5 m (intermediate-low), 1.2 m (intermediate-high), and 2.0 m (highest) based on different degrees of ocean warming and ice sheet loss.

In addition to SLR, researchers have also reached a consensus on future changes in TC intensity. The heat content stored in the upper ocean provides the energy that fuels the development of TCs. As a result, increased sea surface temperature creates a more favorable environment for TC formation and growth. Emanuel [13] created an index of the potential destructiveness of TCs, based on total power dissipation integrated over a TC's entire lifetime. Emanuel used this index to study hurricanes of the past 30 years and found that the index has increased significantly since the mid-1970s [13]. Webster et al. [14] examined the intensity of tropical cyclones for more than 35 years in the context of increasing sea surface temperature and found that the number of category 4 and 5 hurricanes increased at different rates in the North Pacific, India, Southwest Pacific, and North Atlantic oceans. According to Mousavi et al. flood elevations caused by catastrophic hurricane storm surges in the Gulf of Mexico will rise by 0.5 m and 1.8 m by the 2030s and 2080s, respectively [15]. Even though uncertainty exists in hurricane pattern change studies, it is certain that storm surge caused by extreme tropical cyclones will be a significant trigger for coastal flooding in the future.

This study will quantify the risk of SMPs' loss of function after being submerged under storm surge and seawater inundation during tropical cyclones, and identify how SLR and more extreme storms in future climate change scenarios can exacerbate the situation.

2. Materials and Methods

2.1. Historical TC-Induced Storm Surge Data

From 1851 to 2018, 243 TCs in 132 years made landfall or caused storm surges on the South Carolina coast. To determine the maximum storm surge heights, all of these storms were simulated using a hydrodynamic model. Figure 1 depicts the locations where each year's simulated maximum storm surge occurred.

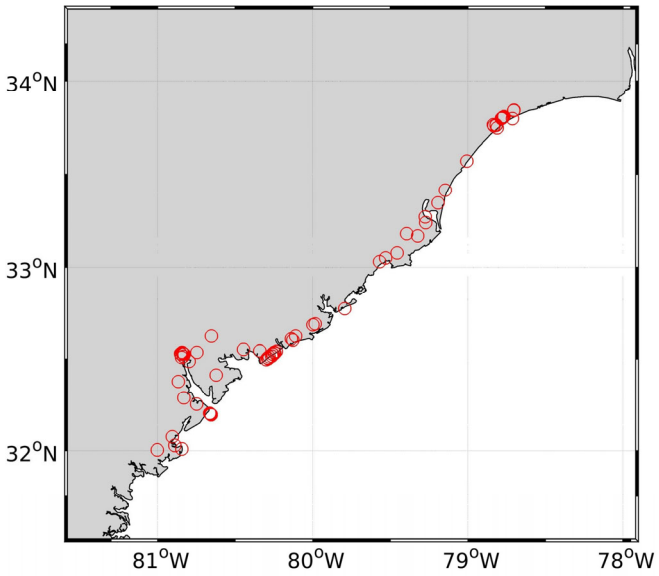

Figure 1. Locations of each years' maximum storm surge height during 1851–2018.

We used the above modeled historical storm surge height data to estimate the storm surge heights for the South Carolina coast with 5-year, 10-year, 50-year, 100-year, and 1000-year return periods. The storm-surge-height return periods were calculated based on the classical Hazen method [16]

$$T_p = \frac{2n}{2m-1} \quad (1)$$

where T_p is the return period of a specific storm surge height, n is the total number of events (132 in this study), and m is the rank of a specific storm surge height. m = 1 when the maximum storm surge height is the 132-year high.

The resultant storm surge height return period is shown in Figure 2. The storm surge heights as a function of return periods fit into $h(t) = -0.0394 + 1.38\ln(t) - 0.107\ln(t)^2$, where h is the storm surge height (in m) and t is the return period (in year).

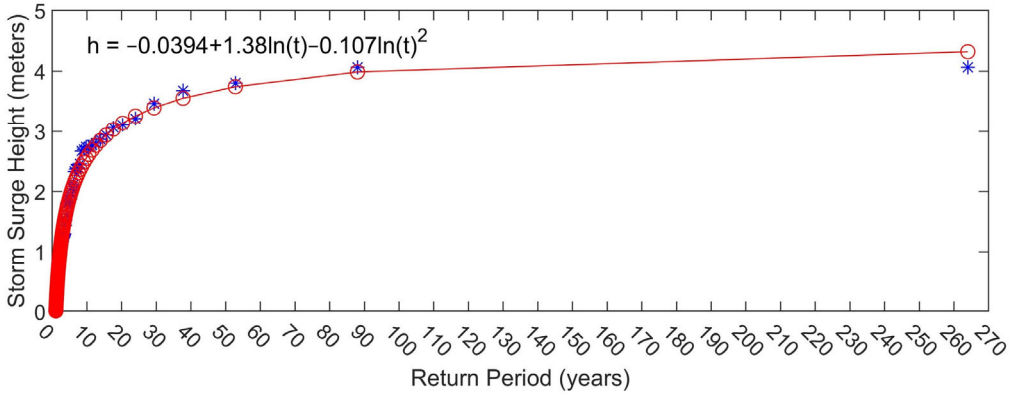

Figure 2. Storm surge height on SC coast as a function of their return periods.

The storm surge heights for the return periods of 5, 10, 50, 100, and 1000 years are 1.9 m, 2.6 m, 3.7 m, 4.0 m, and 4.4 m, respectively. The 1000-year storm surge height has never occurred before and its value is extrapolated from past storm surge records. Note that these storm surge modeling results were based solely on changes in water level caused by TCs. Astronomical tide is another important factor affecting the actual storm surge height. For example, the once-in-100-years (return period = 100 years) storm surge height for the South Carolina coast is 4.0 m, which may coincide with a high tide of 1.5 m—the average high tide for the South Carolina coast—and become 5.5 m, or coincide with a low

tide of −1.5 m and become 2.5 m, or coincide with a tide somewhere between the two extremes. Due to the uncertain possibilities of the tidal phase coinciding with storm surge height, the astronomical tide-caused water level changes are not included in the calculation of the storm-surge-height return periods. Instead, the impact of tides is considered as a worst-case scenario in the subsequent inundation modeling and the assessment of the risks of SMPs, in which case it is assumed that the storm surge height with a certain return period coincides with a high tide.

2.2. Inundation

The method for calculating inundation extent as a result of storm surge during a tropical cyclone is illustrated in Figure 3. While storm surge heights caused by past tropical cyclones were simulated using the coupled hydrodynamic model, inundation areas were calculated based on the geographic information system (GIS) technique using the QGIS platform. It is well established that storm surge height intrudes on land with decay [17]. The surge decay coefficient (*SDC*) is defined as follows:

$$SDC = \frac{H_s - H_i}{W_i - W_c} \quad (2)$$

where H_s is the storm surge height, H_i is inundation elevation (the average elevation where the effect of the surge can reach), W_i is inundation width (the longest distance of inundated area away from coast), and W_c is the width of the constant surge from the coast.

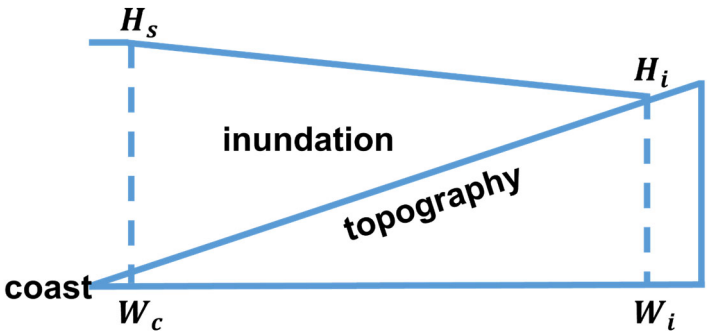

Figure 3. Illustration of calculation of inundation area using storm surge height and topography.

We assume that the inundation begins at the coastline so that W_c = 0 m. We first run an idealized 2D hydrodynamic model simulation by setting sea level to the storm surge heights (the H_s in Equation (2)) of 1.9 m, 2.6 m, 3.7 m, 4.0 m, and 4.4 m to determine the widths of the inundated area W_i and the end inundation elevation H_i. The widths of the inundated area and the end inundation elevation were obtained manually based on flooding extent maps produced by the hydrodynamic model Delft3D-FLOW.

Delft3D-FLOW is a 2D or 3D simulation program that calculates water's non-steady flow and transport caused by tidal and meteorological forcing on a rectilinear or a curvilinear fitted grid. The spatial resolution varies from 127 to 1268 m in the x direction and 55 to 557 m in the y direction. The time step is 0.4 s. Such grid spacing and time step allow stable integration in shallow water, e.g., when the water depth is 100 m, the Courant number is dt/(dx/sqrt(gH)) = 0.2, which is much smaller than required for computational stability under CFL conditions. The Holland model [18] is used to create the wind data based on hurricane track and intensity to drive Delft3D-FLOW.

The SDC values can then be determined based on the above equation. Additionally, later, these SDCs were applied to the inundation area calculation under different SLR scenarios using the geographic information system technique on the QGIS platform, which is more computationally efficient than numerically modeling each individual scenario. The QGIS Geospatial Data Abstraction Library (GDAL) was used to process the inundation

maps. The steps for determining whether a giver inland location is inundated are as follows:

1. Calculate the raster distance (*RD*) from the coastline to the inland location using the Proximity function. Note *RD* = 0 m at the coastline.
2. Determine the water depth (*WD*) based on H_s, *SDC*, *RD*, and DEM elevation (*DEM*) using the formula: $WD = (H_s - RD \times SDC) - DEM$.
3. *WD* > 0 indicates inundation. The Raster calculator function in QGIS is used in this step.

The storm surge height, inundation width, the inundation elevation, and surge decay coefficient for storm surges with different return periods are listed in Table 1.

Table 1. Storm surge height, inundation width, end inundation elevation, and surge decay coefficient for different return periods.

Return Period (Year)	Surge Height Hs (m)	Inundation Width Wi (m)	Inundation Elevation Hi (m)	Surge Decay Coefficient (SDC)
5	1.9	764	1	0.0012
10	2.6	1062	1.4	0.0011
50	3.7	1337	1.8	0.0014
100	4	1417	2.1	0.0014
1000	4.4	1500	2.1	0.0015

2.3. Experiments—Impact of SLR to Stormwater Ponds

For each return period of storm surge height, the inundation is calculated under the following scenarios: (1) no tide and no SLR; (2) with tide and no SLR; (3) with tide and SLR = 0.5 m; (4) with tide and SLR = 1.0 m; (5) with tide and SLR = 1.5 m; and (6) with tide and SLR = 2.0 m. These SLR scenarios include the low-, intermediate–low-, intermediate–high-, and high-risk scenarios proposed by Parris [12]. A total of 36 calculations (6 TC storm surge return periods each under 6 different SLR scenarios) were carried out. In each calculation, the number of submerged SMPs was counted. The impact of SLR scenarios on the number of SMPs affected during non-storm (return period of zero years) and storm conditions (return periods of 5, 10, 50, 100, and 1000 years) were assessed. The high-risk "hotspots" were identified where mitigation and adaptation efforts are required under future climate SLR scenarios.

Furthermore, the South Carolina coast was divided into three domains based on topography and the three SMP clusters centered in these three regions: Long Bay, Charleston, and Beaufort. In addition to the assessment of the entire South Carolina coast as a single domain, the impact of SLR on SMPs was also evaluated in detail for each of these three domains individually. Note that some SMPs are outside of these three regions.

2.4. Storm Water Pond and Topography Data

The South Carolina storm management pond survey [19] based on aerial images, which identified approximately 21,594 SMPs, was used in this study for the SMP locations (Figure 4). The aerial images used to identify SMPs are provided by the National Agriculture Imagery Program (NAIP). The spatial resolution of these aerial images is about 1 m. The SMPs are concentrated in three high-density clusters in the Long Bay, Charleston, and Beaufort areas. These topography data are an important input for producing the inundation area. The topography data used in this study were obtained from the United States Geological Survey 3D Elevation Program (3DEP), with a spatial resolution of 30 m.

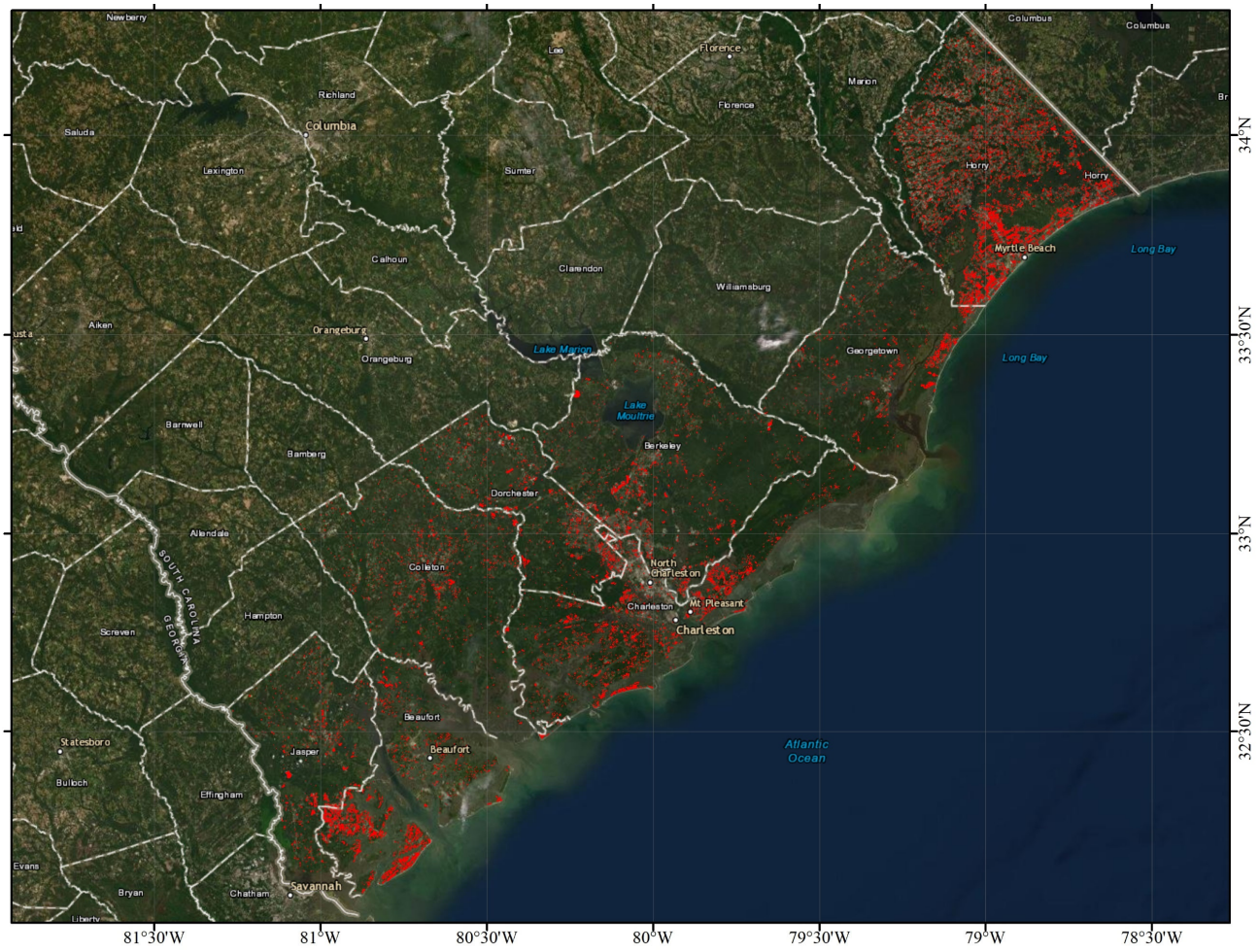

Figure 4. Stormwater management ponds in South Carolina.

3. Results

3.1. Long Bay

Figure 5 shows the number of SMPs in the Long Bay region that are vulnerable to TC storm surges with 0-year (non-storm), 5-year, 10-year, 50-year, 100-year, and 1000-year return periods under 0 m, 0.5 m, 1.0 m, 1.5 m, and 2.0 m SLR scenarios. A non-storm high tide could inundate 29 SMPs under current climate conditions. For stronger hurricanes, the number could rise sharply, reaching about 300 SMPs for a 100-year TC storm surge. However, SMPs at risk of 100-year and 1000-year storm surges appear to be similar. When the tide is not included, the number is significantly lower, emphasizing the importance of taking tides into account. The worst-case scenario method is used, which involves adding an average high tide to the storm surge heights for all return periods.

Unsurprisingly, more SMPs would be at risk of TC storm surges under future SLR scenarios. According to Figure 5, under a non-storm condition, the number of affected SMPs would double from 29 to 54, with an SLR of 0.5 m. The number of affected SMPs continues to grow linearly reaching 157 with an SLR of 2 m. Under storm conditions, the number of affected SMPs also increases almost linearly with SLR. For the Long Bay area, each 0.5 m SLR would expose about 50 more SMPs to TC storm surge and inundation. Note that the number of affected SMPs listed above does not represent the total number of SMPs that will be inundated when a single hurricane hits the SC coast to cause storm surge and inundation at an arbitrary location. It is instead the number of SMPs that could be inundated by a local storm surge.

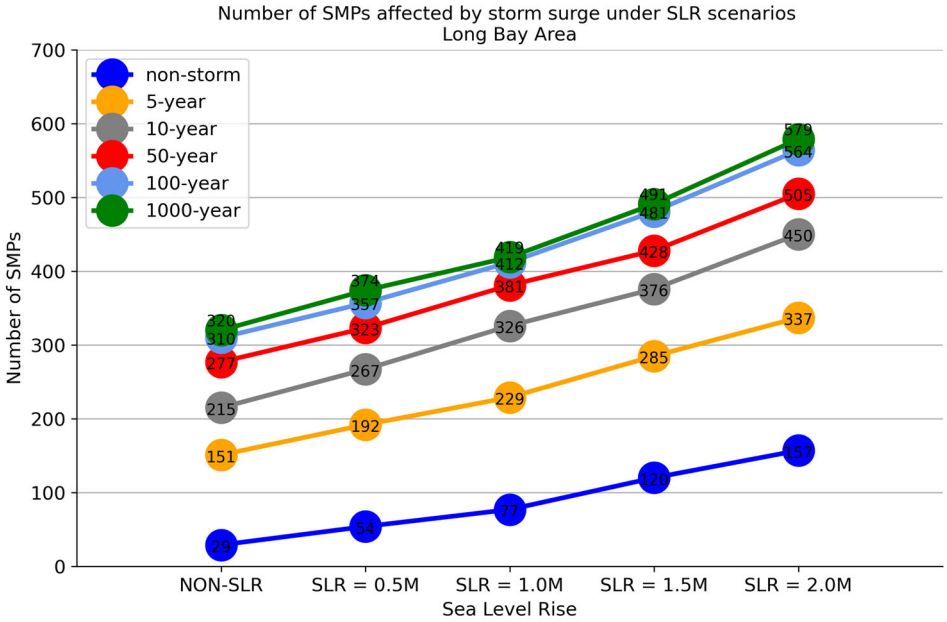

Figure 5. The number of SMPs in Long Bay region that are at risk of storm surges with 0-year (non-storm), 5-year, 10-year, 50-year, 100-year, and 1000-year return periods under scenarios of 0 m, 0.5 m, 1.0 m, 1.5 m, and 2.0 m SLR.

Figure 6 depicts the inundation map for the Long Bay area caused by hurricanes with different return periods under an SLR = 2.0 m scenario. The green–yellow colors indicate topography above sea level, and the blue–red colors represent the water depth, which includes perennial wet areas (rivers and wetlands) as well as the flooded areas. More areas are inundated when the storm surge heights increase from non-storm to 5-, 10-, 50-, 100- and 1000-year return periods, as indicated by the increase in the blue–red areas. Under non-storm conditions, SMPs in several locations along the coast of Long Bay immediately adjacent to the coastline are vulnerable to high tides. As the storm surge height increases, several high-risk hotspots become evident: the SMPs near Winyah Bay, particularly those near Georgetown City and Parleys Island, are at the greatest risk, as indicated by the clustering of the black-shaded areas. Note that Figure 6 has been rotated clockwise toward the northeast.

3.2. Charleston

Figure 7 shows the number of SMPs in the Charleston region that are vulnerable to submersion from TC storm surge heights with 0-year (non-storm), 5-year, 10-year, 50-year, 100-year, and 1000-year return periods under scenarios of 0 m, 0.5 m, 1.0 m, 1.5 m, and 2.0 m SLR. A non-storm high tide could threaten ~56 SMPs under current climate conditions. The number might increase sharply for stronger TCs, reaching more than 400 SMPs for a 100-year storm surge. However, the number of SMPs at risk of a 100-year storm surge and a 1000-year one appears to be similar. The worst-case scenario method is used for the Long Bay region, where an average high tide is added to the storm surge heights for all return periods. Overall, the SMPs in the Charleston area are more vulnerable to high tides and TC-caused storm surges than those in the Long Bay area, mainly due to the low-lying terrain of the Charleston Harbor area.

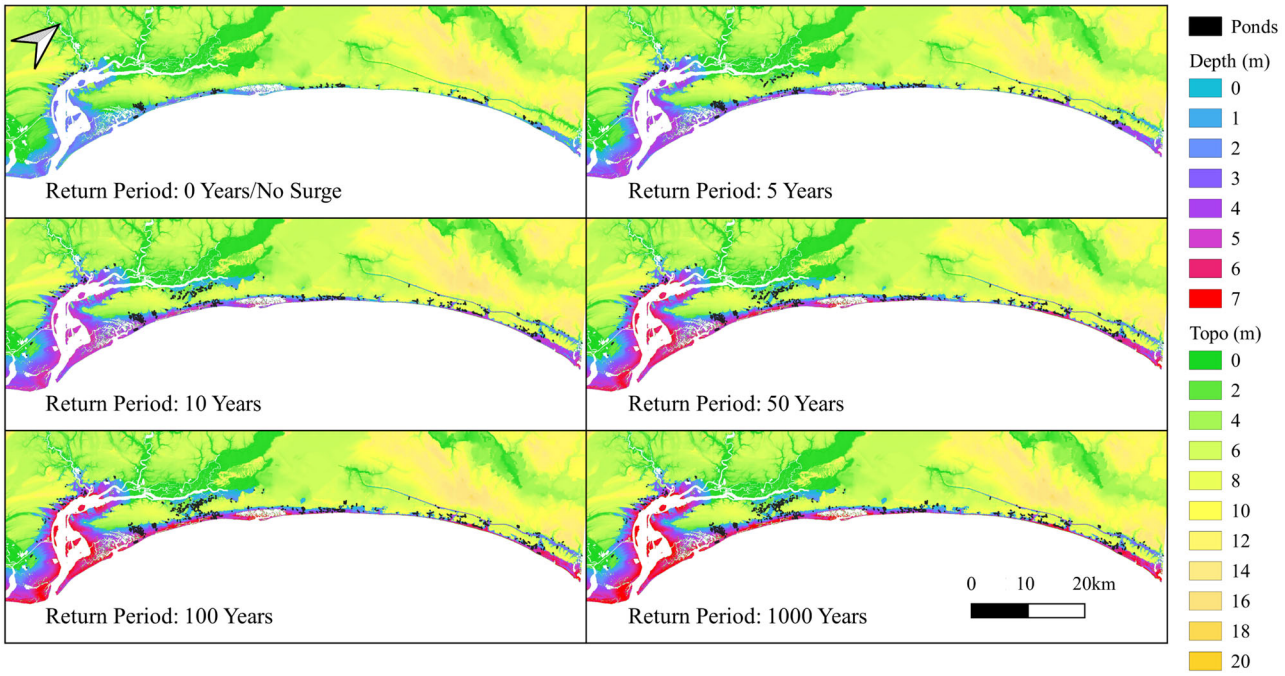

Figure 6. Long Bay area inundation map (blue–red) caused by storm surge heights with different return periods under an SLR scenario of 2.0 m. The SMPs at risk are marked as black shades.

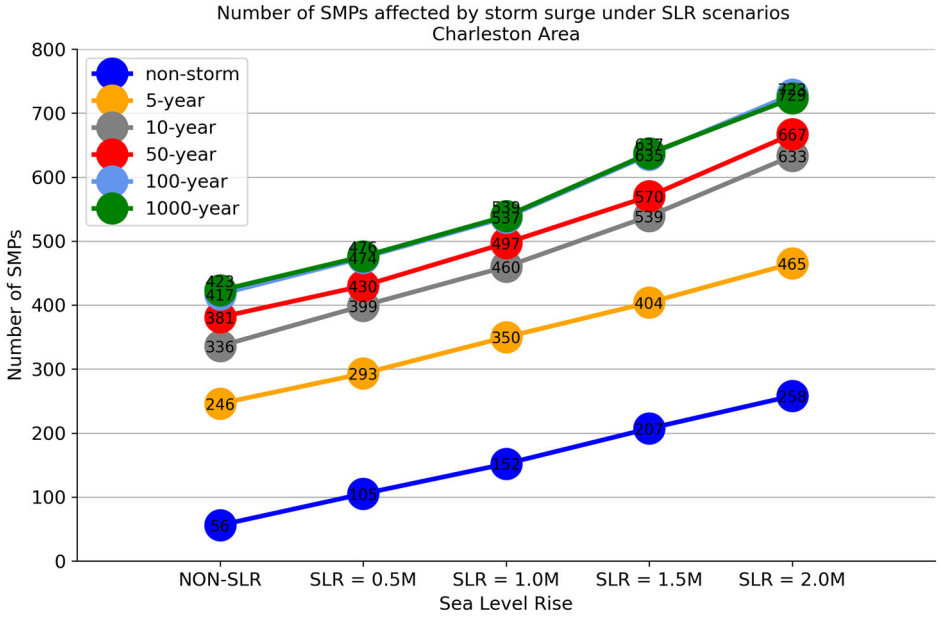

Figure 7. The number of SMPs in Charleston Harbor that are at risk of storm surge heights with 0-year (non-storm), 5-year, 10-year, 50-year, 100-year, and 1000-year return periods under scenarios of 0 m, 0.5 m, 1.0 m, 1.5 m, and 2.0 m SLR.

In Charleston Harbor, similar to Long Bay, more SMPs would be vulnerable to TC storm surges under future SLR scenarios. According to Figure 7, with an SLR of 0.5 m, the number of affected SMPs would double from 56 to 105 under non-storm high-tide conditions. The number would keep rising almost linearly, reaching 258 with an SLR of 2 m. The number of vulnerable SMPs also increases almost linearly with SLR during TC storm surges. In the Charleston Harbor area, there would be about 70 more SMPs at risk of storm surge and inundation for every 0.5 m SLR.

Figure 8 depicts the inundation map for the Charleston Harbor area caused by TC storm surges under an SLR of 2.0 m. The green–yellow colors represent topography above sea level, and the blue–red colors represent the water depth, including perennially wet areas and flooded areas, i.e., areas that were previously dry but became wet during the TC storm surges. As shown by the increase in blue–red areas, when storm surge heights increase from non-storm to 5-, 10-, 50-, 100-, and 1000-year return periods, more areas and SMPs are inundated. The majority of SMPs in the Charleston area are located around the Charleston Harbor, and few are immediately adjacent to the coastline. SMPs in several locations around Charleston Harbor are at risk of non-storm high tides. As the TC storm surge height rises, one hotspot becomes evident: the SMPs near Mount Pleasant. Note that Figure 8 has also been rotated clockwise toward the northeast.

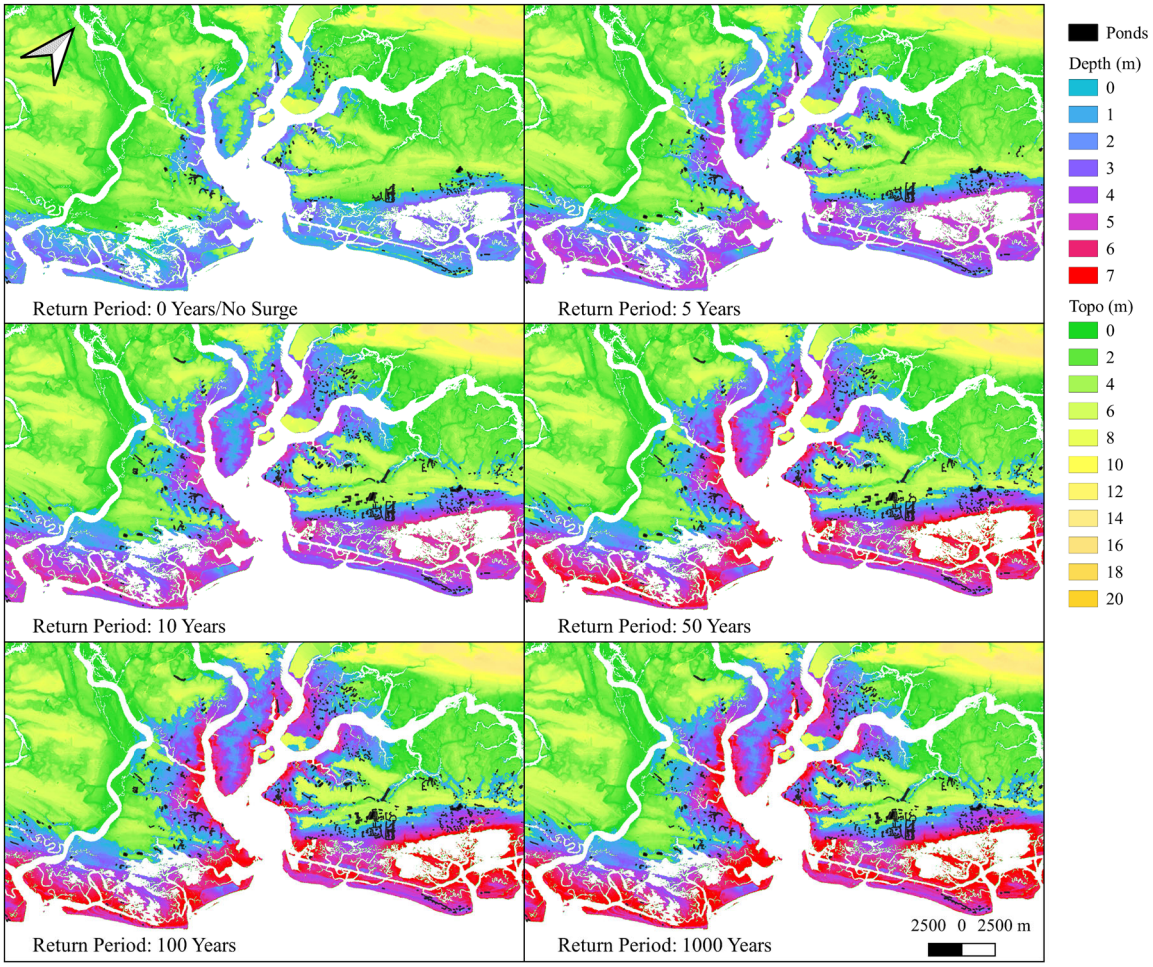

Figure 8. Charleston area inundation map (blue–red) caused by storm surge heights with different return periods under an SLR scenario of 2.0 m. The SMPs at risk are shaded black.

3.3. Beaufort

Figure 9 shows the number of SMPs in Beaufort County at risk of TC storm surges with 0-year (non-storm), 5-, 10-, 50-, 100-, and 1000-year return periods under 0 m, 0.5 m, 1.0 m, 1.5 m, and 2.0 m SLR scenarios. A non-storm high tide could inundate ~69 SMPs in the current climate. The number rises for stronger storm surges, reaching more than 700 SMPs for a 100-year storm surge. Notably, 100-year and 1000-year TC storm surges appear to expose similar numbers of SMPs. Again, the worst-case scenario method adds a high tide to the storm surge heights for all return periods. In the Beaufort area, there are significantly more vulnerable SMPs than in the Long Bay area and Charleston Harbor area, mainly due to its low-lying terrain.

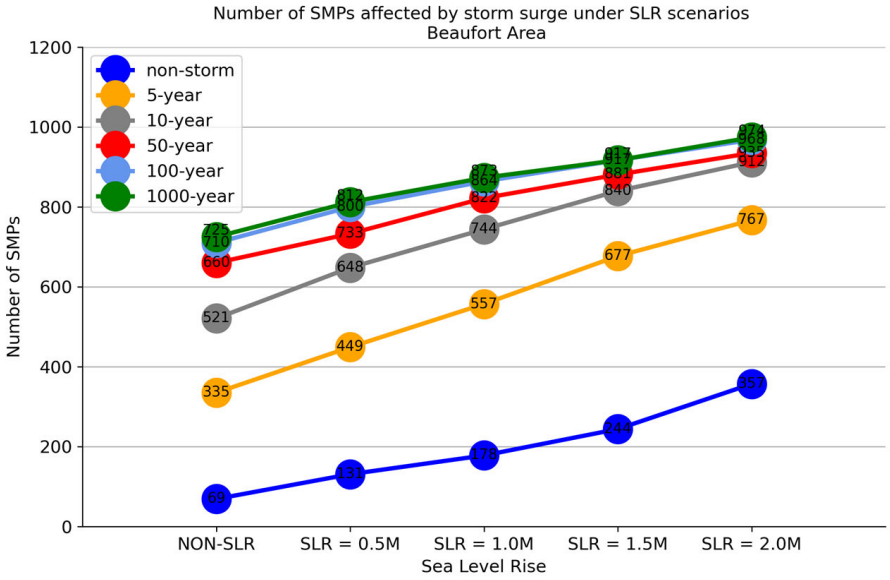

Figure 9. Beaufort area number of SMPs at risk of storm surge height with 0-year (non-storm), 5-year, 10-year, 50-year, 100-year, and 1000-year return periods under scenarios of 0 m, 0.5 m, 1.0 m, 1.5 m, and 2.0 m SLR.

Similar to the other two regions, more SMPs would be at risk of storm surges under future SLR scenarios in Beaufort County. Figure 9 shows that an SLR of 0.5 m would double the number of SMPs that are affected by high tides from 69 to 131, and with an SLR of 2 m, the number would reach 357. Under TC storm surge conditions, the number of affected SMPs also increases almost linearly with SLR. For every 0.5 m SLR, 80 more SMPs in Beaufort would be at risk of TC storm surge and inundation.

Figure 10 shows the inundation maps for Beaufort County area caused by TC storm surges under an SLR of 2.0 m. Unsurprisingly, when storm surge heights increase from non-storm to 5-, 10-, 50-, 100-, and 1000-year return periods, more areas are inundated. Beaufort County's SMPs, unlike those in Charleston Harbor, concentrate on the Hilton Head Island immediately adjacent to the coastline. The SMPs on Hilton Head Island along the coast are at risk during non-storm high tides, and they have higher risks as storm surge height rises: even a mild 5-year TC storm surge would submerge nearly half of Hilton Head Island's SMPs.

3.4. South Carolina

Figure 11 shows the number of South Carolina SMPs at risk of TC storm surges with various return periods under SLR scenarios. A non-storm high tide could inundate ~208 SMPs in the current climate. The number increases sharply for stronger hurricanes, reaching 1700 SMPs for a 100-year TC storm surge. The SMPs at risk of 100- and a 1000-year TC storm surges appear similar. Under future SLR scenarios, more SMPs would be vulnerable to TC storm surges. Figure 11 shows that with an SLR of 0.5 m, the number of affected SMPs would double from 208 to 405 for non-storm high tides. The number continues to rise almost linearly, reaching 998 with a 2 m SLR. Under storm conditions, the number also increases linearly with SLR. For every 0.5 m SLR, 200 more South Carolina SMPs would be at risk from storm surge and inundation, or 10 more SMPs for every inch of SLR.

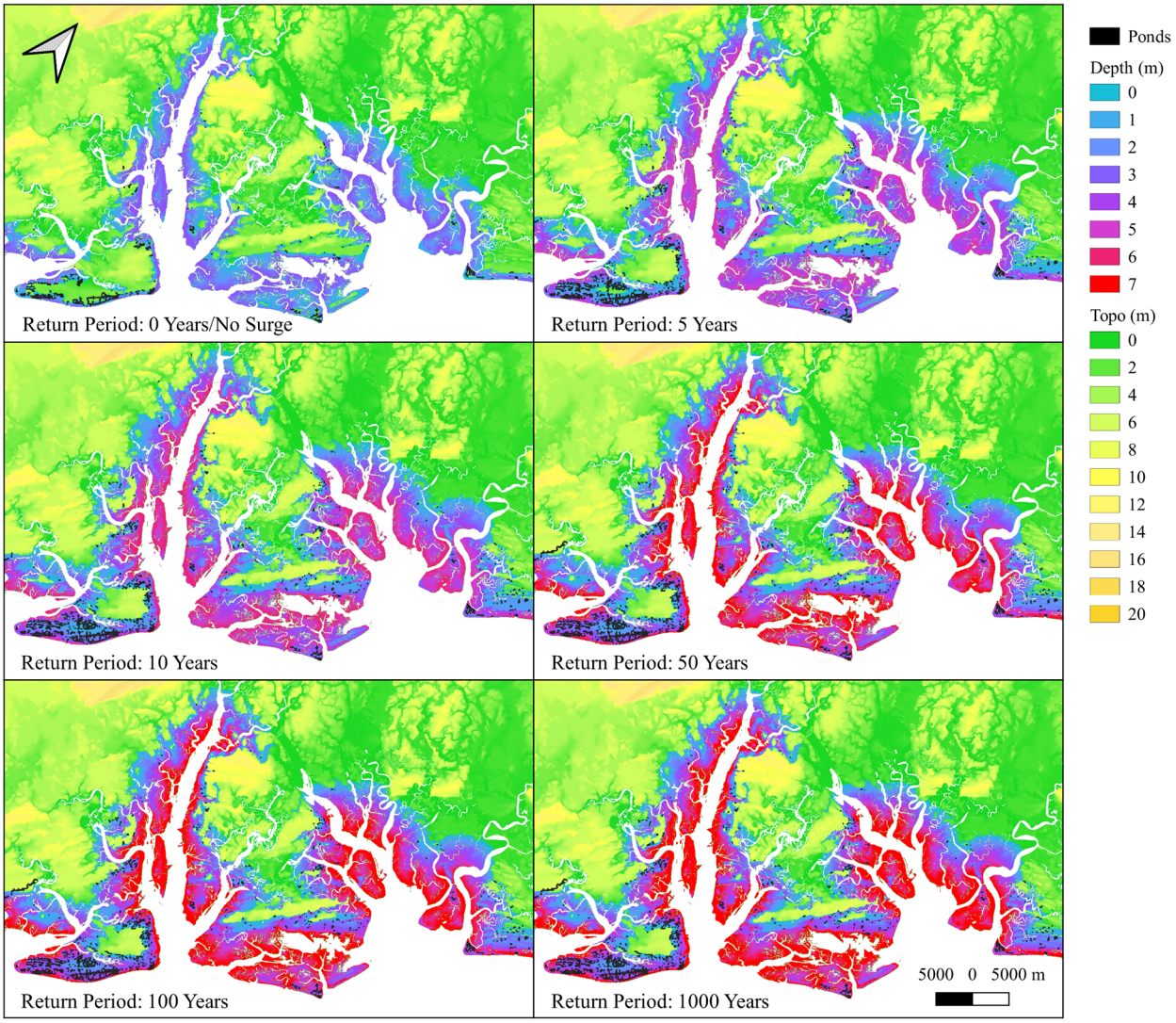

Figure 10. Beaufort County area inundation map (blue–red) caused by storm surge heights with different return periods under an SLR scenario of 2.0 m. The SMPs at risk are shaded black.

Under the worst-case scenario, 2600 SMPs could be inundated if a local 1000-year TC storm surge coincides with a high tide under an SLR of 2 m, or 12% of all SMPs in South Carolina, according to the 2014 survey (Cotti-Rausch et al., 2018).

Figure 12 shows SMPs at risk of TC storm surges with different return periods under an SLR = 2.0 m scenario. The danger zone hotspots identified in Figures 6, 8 and 10 are also evident in Figure 12, including Hilton Head Islands (Beaufort County), Mount Pleasant (Charleston area), and Pawleys Island (Long Bay). In addition to these hotspots, SMPs in Kiawah Island, between Charleston Harbor and Beaufort County, also have a high risk of being inundated by storm surges under SLR scenarios.

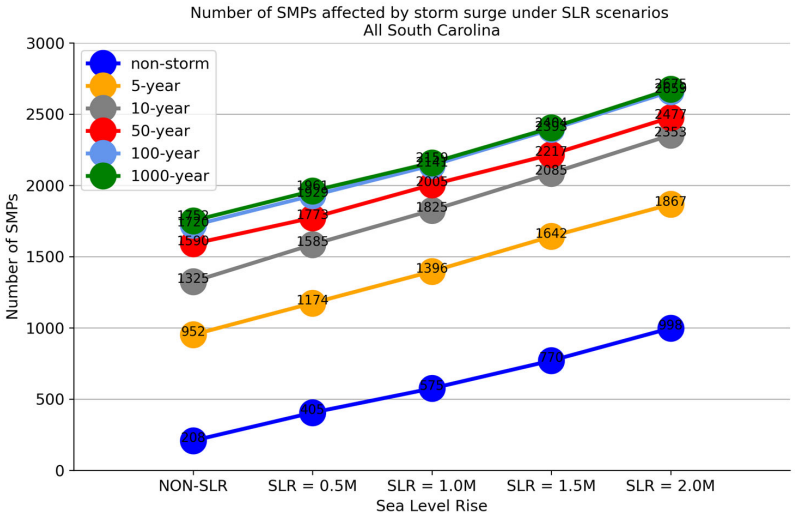

Figure 11. The number of SMPs in the entire coast of South Carolina that are at risk of storm surge heights with 0-year (non-storm), 5-year, 10-year, 50-year, 100-year and 1000-year return periods under scenarios of 0 m, 0.5 m, 1.0 m, 1.5 m, and 2.0 m SLR.

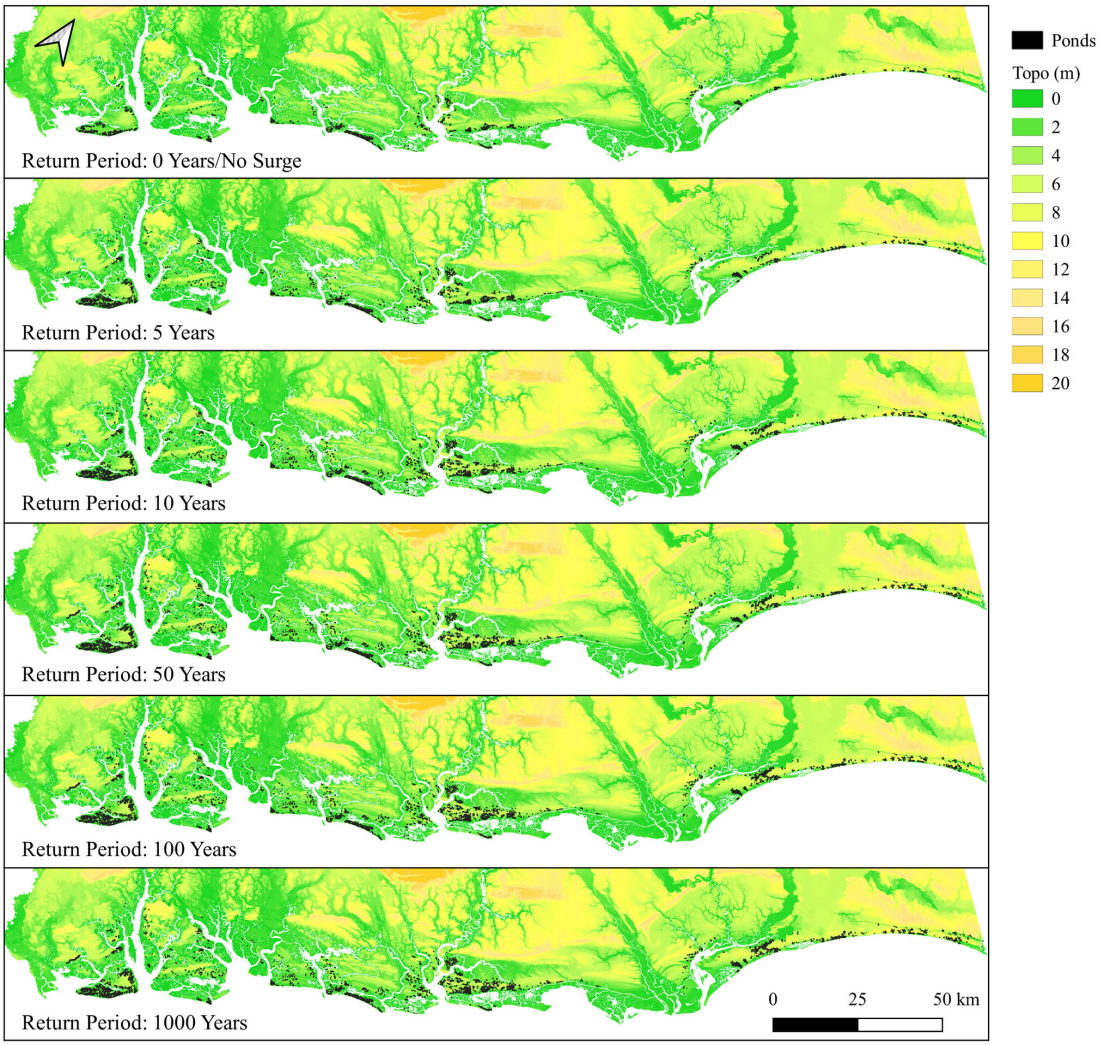

Figure 12. Map of SMPs at risk of storm surges for all of South Carolina, with different return periods under an SLR scenario of 2.0 m. The SMPs at risk are shaded black.

4. Discussion

The result of this study inevitably contains uncertainties. The 30 m topography data, for example, may be too coarse for some SMPs to be resolved accurately. Furthermore, we used the high-tide water levels to represent the effect of astronomical tides during storm surges, which may overestimate the storm surge water level and the hence the damage caused by the storm surge to the SMPs. As a result of these uncertainties, the findings of this study should be used with caution and interpreted as a general trend of aggravated threats to SMPs from climate change, such as sea level rise and more extreme tropical cyclones, rather than an accurate prediction of which storm pounds will be damaged in any given storm.

5. Conclusions

Tropical cyclone-induced storm surges cause inundation that could threaten the proper function of stormwater management ponds in the coastal South Carolina area, and the risks could be aggravated by future sea level rise.

A framework is developed to assess the impact of TC-induced storm surges and inundation on stormwater management ponds. A hydrodynamic model simulates storm surges caused by historical hurricanes that struck the coast of South Carolina between 1851 and 2018. Storm surge heights with various return periods are established. Inundation caused by tides and storm surges could threaten storm management ponds in coastal regions. The rise in sea level could exacerbate these risks. Under various SLR scenarios, the inundations caused by storm surge heights with return periods of 0 (non-storm high tides), 5, 10, 50, 100, and 1000 years are simulated, and the SMPs at risk of being affected by these events are counted. For the entire South Carolina region, the number of SMPs at risk of being inundated by tides and storm surges would increase almost linearly with SLR by around 10 SMPs for every inch of SLR, for TC storm surges with all return periods.

Three coastal regions—Long Bay, Charleston, and Beaufort—are analyzed in detail to identify the communities whose SMPs are at high risk in the face of future SLR scenarios. Hilton Head Islands, Charleston Harbor, Kiawah Island, George Town City, and Pawleys Island are identified as these high-risk hotspot areas. If submerged by storm surge and seawater inundation, current SMPs installed in South Carolina could be incapable of functioning to mitigate the increased surface runoff and flash flooding caused by extreme rainfalls. Therefore, the findings of this study provide necessary information regarding the locations where current SMPs must be re-designed and where more SMPs must be developed. The modeling and analysis system developed for this study can be applied to assess the impact of SLR and other climate change scenarios on SMP facilities in other regions.

Author Contributions: Investigation, H.Z. and D.S.; conceptualization, S.B., L.P., P.T.G. and H.M.; validation, H.Z. and D.S.; methodology, D.S., L.P. and P.T.G.; project administration, S.B. and H.M.; funding acquisition, S.B. and H.M.; software, D.S.; supervision, S.B.; writing—draft preparation, D.S.; writing—review and editing, H.Z. All authors have read and agreed to the published version of the manuscript.

Funding: This research was funded by South Carolina Sea Grant Consortium grant number NA140AR 4170088, NOAA grant number NA22NWS4320003, and National Science Foundation's Major Research Instrumentation program grant number AGS-1624068.

Institutional Review Board Statement: Not applicable.

Informed Consent Statement: Not applicable.

Data Availability Statement: Data is contained within the article.

Acknowledgments: This project was funded by the South Carolina Sea Grant Consortium grant NA140AR4170088. The work on storm surge and flooding modeling was also partially supported by the NOAA grant NA22NWS4320003 awarded through the Cooperative Institute for Research to Operations in Hydrology (CIROH). The computation facility was provided by the National Science Foundation's Major Research Instrumentation program under grant AGS-1624068.

Conflicts of Interest: The authors declare no conflict of interest.

References

1. Chen, C.-N.; Tsai, C.-H.; Tsai, C.-T. Reduction of discharge hydrograph and flood stage resulted from upstream detention ponds. *Hydrol. Process.* **2007**, *21*, 3492–3506. [CrossRef]
2. Sahoo, S.N.; Pekkat, S. Detention ponds for managing flood risk due to increased imperviousness: Case study in an urbanizing catchment of India. *Nat. Hazards Rev.* **2018**, *19*, 05017008. [CrossRef]
3. Chrétien, F.; Gagnon, P.; Thériault, G.; Guillou, M. Performance analysis of a wet-retention pond in a small agricultural catchment. *J. Environ. Eng.* **2016**, *142*, 04016005. [CrossRef]
4. Hancock, G.S.; Holley, J.W.; Chambers, R.M. A Field-Based Evaluation of Wet Retention Ponds: How Effective Are Ponds at Water Quantity Control? *JAWRA J. Am. Water Resour. Assoc.* **2010**, *46*, 1145–1158. [CrossRef]
5. Lambeck, K.; Chappell, J. Sea level change through the last glacial cycle. *Science* **2001**, *292*, 679–686. [CrossRef] [PubMed]
6. Severinghaus, J.P.; Brook, E.J. Abrupt climate change at the end of the last glacial period inferred from trapped air in polar ice. *Science* **1999**, *286*, 930–934. [CrossRef] [PubMed]
7. Marshall, S.J.; Clarke, G.K.C. Modeling North American freshwater runoff through the last glacial cycle. *Quat. Res.* **1999**, *52*, 300–315. [CrossRef]
8. Oppenheimer, M.; Little, C.M.; Cooke, R.M. Expert judgement and uncertainty quantification for climate change. *Nat. Clim. Chang.* **2016**, *6*, 445–451. [CrossRef]
9. Santamaría-Gómez, A.; Gravelle, M.; Dangendorf, S.; Marcos, M.; Spada, G.; Wöppelmann, G. Uncertainty of the 20th century sea-level rise due to vertical land motion errors. *Earth Planet. Sci. Lett.* **2017**, *473*, 24–32. [CrossRef]
10. Van Vuuren, D.P.; Edmonds, J.; Kainuma, M.; Riahi, K.; Thomson, A.; Hibbard, K.; Hurtt, G.C.; Kram, T.; Krey, V.; Lamarque, J.-F.; et al. The representative concentration pathways: An overview. *Clim. Chang.* **2011**, *109*, 5–31. [CrossRef]
11. Griffiths, J.A.; Zhu, F.; Chan, F.K.S.; Higgitt, D.L. Modelling the impact of sea-level rise on urban flood probability in SE China. *Geosci. Front.* **2019**, *10*, 363–372. [CrossRef]
12. Parris, A.S.; Bromirski, P.; Burkett, V.; Cayan, D.R.; Culver, M.E.; Hall, J.; Horton, R.M.; Knuuti, K.; Moss, R.H.; Obeysekera, J. *Global Sea Level Rise Scenarios for the United States National Climate Assessment*; Tech Memo OAR CPO-1; United States Department of Commerce, National Oceanic and Atmospheric Administration: Washington, DC, USA, 2012.
13. Emanuel, K. Increasing destructiveness of tropical cyclones over the past 30 years. *Nature* **2005**, *436*, 686–688. [CrossRef] [PubMed]
14. Webster, P.J.; Holland, G.J.; Curry, J.A.; Chang, H.-R. Changes in tropical cyclone number, duration, and intensity in a warming environment. *Science* **2005**, *309*, 1844–1846. [CrossRef] [PubMed]
15. Mousavi, M.E.; Irish, J.L.; Frey, A.E.; Olivera, F.; Edge, B.L. Global warming and hurricanes: The potential impact of hurricane intensification and sea level rise on coastal flooding. *Clim. Chang.* **2011**, *104*, 575–597. [CrossRef]
16. Hazen, A. *Flood Flows: A Study of Frequencies and Magnitudes*; John and Wiley & Sons: Hoboken, NJ, USA, 1930.
17. Rana, M.S.; Gunasekara, K.; Hazarika, M.K.; Samarakoon, L.; Siddiquee, M. Application of remote sensing and GIS for cyclone disaster management in coastal area: A case study at Barguna district, Bangladesh. *Int. Arch. Photogramm. Remote Sens. Spat. Inf. Sci.* **2010**, *38*, 122–126.
18. Holland, G.J. An Analytic Model of the Wind and Pressure Profiles in Hurricanes. *Monthly Weather Rev.* **1980**, *108*, 1212–1218. [CrossRef]
19. Cotti-Rausch, B.E.; Majidzadeh, H.; DeVoe, M.R.; South Carolina Sea Grant Consortium. *Stormwater Ponds in Coastal South Carolina: 2018 State of Knowledge Report Executive Summary*; South Carolina State Documents Depository: Dallas, TX, USA, 2018.